

Attachment #2

#### ABOUT THE COVER

The author gratefully acknowledges the cover photograph by Felice Frankel, a physicist in Residence at the Massachusetts Institute of Technology and coauthor of *On the Surface of Things: Images of the Extraordinary in Science*.

This particular image, taken with Nomarski optics, presents a wafer-bonded piezoresistive pressure sensor. It is fabricated in the sealed-cavity process developed by Professor Martin Schmidt of the Massachusetts Institute of Technology with his graduate students, Lalitha Parameswaran and Charles Hsu. The piezoresistors are clearly visible, and the slight contrast across the central diaphragm region shows that the diaphragm is actually slightly bent by the pressure difference between the ambient and the sealed cavity beneath.

---

## MICROSYSTEM DESIGN

Stephen D. Senturia  
*Massachusetts Institute of Technology*



KLUWER ACADEMIC PUBLISHERS  
Boston / Dordrecht / London

BEST AVAILABLE COPY

Figure 20.19 illustrates the procedure. If we assume a tensile (positive) stress  $\sigma_n$  in the nitride prior to release, and a compressive stress  $-\sigma_a$  in the aluminum prior to release, then bond the two layers together and release them, the interface moves to the right by an amount  $\delta$ . To find delta, we require that the tension be equal in the two parts of the beam. This leads to

$$\delta = \frac{L}{2} \frac{\sigma_a h_a p (1-p)}{E_a h_a (1-p) + E_n h_n} \quad (20.48)$$

From this, the stress in the uncoated nitride is

$$\sigma_{n,final} = \frac{E_n h_n \sigma_n + p E_n h_a \sigma_a + (1-p) E_a h_a \sigma_n}{E_n h_n + (1-p) E_a h_a} \quad (20.49)$$

and the final tension in the beam is then  $W h_n \sigma_{n,final}$ . Using this result, Payne calculates the Rayleigh-Ritz resonant frequency as

$$\omega = \sqrt{10} \left[ \frac{h_n [E_n h_n \sigma_n + p E_n h_a \sigma_a + (1-p) E_a h_a \sigma_n]}{[E_n h_n + (1-p) E_a h_a] \left[ h_n \rho_n + p^3 \left( \frac{3p^2}{8} - \frac{15p}{8} + \frac{5}{2} \right) h_a \rho_a \right]} \right]^{1/2} \quad (20.50)$$

Measurements were made on beams of length 200  $\mu\text{m}$  with varying values of  $L_d$ . The beam was excited strongly into resonance by a sinusoidal excitation which was tuned to get a large amplitude. The sinusoid was then turned off and the free oscillation was measured by sensing the diffracted signal. The resulting data were fitted to a damped sinusoid and the resonance frequency was extracted. As expected, the resonant frequency decreased with increasing  $L_d$ , consistent with a compressive stress on the aluminum. The fit of the frequency-vs- $L_d$  data to the above expression permitted extraction of values of  $801 \pm 2$  MPa for the tensile nitride stress, and  $-92 \pm 8$  for the compressive aluminum stress.<sup>7</sup> With these values in hand, it is possible to design the pixel to achieve a desired voltage-displacement characteristic.

<sup>7</sup>These values are the uniaxial stress values after release. Prior to release, the biaxial stress would be larger by a factor  $1/(1-\nu)$ .

#### 20.4.3.4 Beam Curvature

We previously analyzed the diffraction assuming that the displaced beams were perfectly flat. In fact, though, the actuated beams bend, as illustrated in Fig. 20.20.

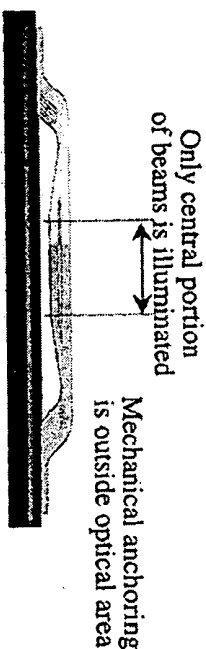


Figure 20.20. Illustrating the bending of GLV beams that occurs during actuation. Only the central portion of the beams is illuminated. [Source: Silicon Light Machines, reprinted with permission.]

In Eq. (20.19), we calculated the deflected shape of a GLV beam assuming perfectly clamped supports. In practice, the supports have finite compliance, but that is a second-order effect. Of more immediate interest is the effect of the beam curvature in the central illuminated portion of the deflected beam. For tension-dominated beams, the bending is nearly perfectly parabolic. We can calculate the radius of curvature from the expression

$$\tilde{w} = Ax(L-x) \quad (20.51)$$

The maximum deflection is at the center, and equals  $AL^2/4$ . In use, this maximum deflection is  $\lambda/4$ . Thus, in use, the largest value of  $A$  is  $\lambda/L^2$ . The radius of curvature is  $1/2A$ . Hence, the most curvature and correspondingly smallest radius of curvature is  $L^2/2\lambda$ . If we use 650 nm as a typical wavelength, and 200  $\mu\text{m}$  as a typical beam length, we estimate the smallest radius of curvature as 3 cm.

If all of the beams, including the reference beams, were similarly curved, then the effect of the curvature would be to focus the diffracted waves. However, the reference beams remain flat, and most of the time, most of the bent beams are deflected far less than the maximum and hence have much larger radii of curvature. This may explain the fact that the curvature of the deflected beams does not appear to create any significant artifact in the projected image [122].

#### 20.4.3.5 Voltage-Intensity Characteristic

We can now assemble the pieces. Substituting  $p = 1$  into Eq. (20.49), corresponding to a fully coated beam, and using the extracted stress values for the individual films, the material densities ( $\rho_a = 2700 \text{ kg/m}^3$ ,  $\rho_n = 3440 \text{ kg/m}^3$ ), elastic moduli ( $E_a = 70 \text{ GPa}$ ,  $E_n = 250 \text{ GPa}$ ), and film thicknesses ( $h_a$